Electrochimica Acta 524 (2025) 146060

Contents lists available at ScienceDirect

Electrochimica Acta

journal homepage: www.journals.elsevier.com/electrochimica-acta

Angle-resolved photoemission spectroscopy and electrocatalysis: is there a bridge in between?

Jan Bosse [a,b], Thomas Lippert [a,b], Andrei Varykhalov [c], Matthias Muntwiler [d], Andrew R. Akbashev [a,*]

[a] PSI Center for Neutron and Muon Sciences, 5232 Villigen PSI, Switzerland
[b] Department of Chemistry and Applied Biosciences, Laboratory of Inorganic Chemistry, ETH Zurich, 8049 Zurich, Switzerland
[c] Helmholtz-Zentrum Berlin für Materialien und Energie, BESSY II, Albert-Einstein-Str. 15, 12489 Berlin, Germany
[d] Center for Photon Science, Paul Scherrer Institute, 5232 Villigen PSI, Switzerland

ARTICLE INFO

Keywords:
ARPES
Oxide
Single crystal
UHV
Electrocatalysis
X-ray
Characterization

ABSTRACT

The electronic interaction between molecules and a surface greatly influences the kinetics of heterogeneous electrocatalytic processes. Here, we explore the possibility of using angle-resolved photoemission spectroscopy (ARPES) to study electrocatalysts. Using oxide materials as an example, we identify pitfalls and key challenges of such experiments and discuss future opportunities.

1. Introduction

Oxide materials show a variety of electronic structures, which makes them the subject of research in two distinct fields: heterogeneous electrocatalysis and condensed matter physics. On the one hand, electronic structure significantly affects the stability of electrosorbed specie and the rate of electrocatalytic reactions on oxide surfaces [1]. On the other hand, oxide materials exhibit a diversity of physical states, ranging from Mott insulator to charge-ordered and superconducting states, which makes them ideal for studying many-body physics and electronic correlations through sophisticated experimental approaches such as inelastic X-ray spectroscopy and angle-resolved photoemission spectroscopy (ARPES). However, as the fields of electrocatalysis and condensed matter physics are rather distinct, the studies of intrinsic physics of oxide systems rarely aim to improve the understanding of electrocatalysis.

The kinetics of electrochemical processes is governed by multiple parameters [2,3]: electronic structure of the surface, molecular configuration and electric field distribution at the electrified electrode-electrolyte interface, thermodynamics of the solvation/desolvation processes and the type of the ion/molecule involved (its chemistry and ionization potential). For oxides, the strength of adsorbate-surface interaction is determined by the electronic properties of a few-nm near-surface layer [1,4], making surface-sensitive techniques essential for their studies. Using ARPES, one can perform a sophisticated analysis of the electronic band structure of the near-surface region and its electronic interaction with adsorbates. Since ARPES requires ultrahigh vacuum (UHV) and cannot be performed *in situ* (i.e. when a surface is covered by an electrolyte), it is important to find a suitable *ex situ* approach that can bridge the results from UHV-based ARPES with the electrochemical response of the surface. Below we discuss the opportunities that ARPES can open for the field of electrocatalysis and the experimental challenges that researchers may face.

2. ARPES for electrocatalysts

Angle-resolved photoemission spectroscopy (ARPES) probes detailed electronic structure of solids, providing information on band dispersions, Fermi surface, band gap, the type and concentration of charge careers, and the interactions between quasiparticles (electrons, phonons) [5]. This technique works as follows: photons with energy greater than the work function illuminate the surface and cause electrons to escape into the vacuum. The kinetic energy of these photoelectrons is measured by the electron analyzer, while the angle of emission reveals

* Corresponding author.
E-mail address: andrei.akbasheu@psi.ch (A.R. Akbashev).

https://doi.org/10.1016/j.electacta.2025.146060
Received 21 August 2024; Received in revised form 22 January 2025; Accepted 15 March 2025
Available online 16 March 2025

their momentum. Using a straightforward formula [6], one can directly extract the band dispersion E(***k***) and Fermi surface from the data. Because ARPES relies on photoemission, it is inherently surface-sensitive. On the one hand, this makes ARPES perfectly suitable for heterogeneous catalysts and electrocatalysts (where the near-surface layer is usually responsible for electron transfer). On the other hand, it means ARPES is highly sensitive to surface contamination and restructuring, which poses major challenges when applying this technique to catalysts where surface is not well-defined at the atomic level. For a deeper dive into this technique, the reader is directed to dedicated reviews [5–7] and the book [8] on ARPES.

Chemical adsorption (chemisorption) at the surface occurs through electron transfer and hybridization [9], playing the key role in electrocatalysis and electrosorption at electrochemical interfaces. As a result of electron transfer, chemisorbed molecules can alter the band structure of a near-surface layer, as reported in studies of adsorption from a gas phase. For example, the surface-adsorbate interaction can induce various changes in the electronic structure, including hybridization of molecular orbitals with metal states [10], a significant reduction of the density of states at the Fermi level of a metal [11], and increased delocalization of the adsorbate's molecular states in particular directions along the surface [12]. Even in the case of physisorption, noticeable changes can occur: for example, Mizushima et al. reported a significant reduction of the Fermi surface volume of the (111) Au Shockley surface states and the formation of large interface electric dipoles upon adsorption [13]. In these studies, photoemission was vital to elucidate the surface-adsorbate interaction. When it comes to (electro) catalysis, fewer studies are available. For example, ARPES studies showed that the Fermi surface of Pt(111) experiences a reconstruction when atomic oxygen is adsorbed on its surface [14]. Specific surface states were shown to participate in weak hybridization between Pt $5d_{xz}$(d_{yz}) and s-/p-orbitals of oxygen, which is likely the factor that leads to a high oxygen reduction reaction activity of Pt. Photoemission measurements also showed that alloying Pt(111) with Ni suppresses surface states in Pt and therefore changes its surface reactivity [15]. As a result, the adsorption of CO on Pt-Ni and Pt-Co induces a smaller energy downshift than in the case of pure Pt(111), implying a weaker adsorption strength for CO on these alloys [16].

The surface of metallic copper is another important example. Studies of adsorption on Cu show possible electronic restructuring of the near-surface layer. For example, completely different changes in electronic structure were observed when iodine and bromine adsorbed on Cu(111): I^- adsorption induced two highly dispersive bands that are parabolic in the entire Brillouin zone within the crystal surface layer, while the adsorption of Br^- created flat and largely hybridized bands [17]. One of the major puzzles with electrocatalysis on Cu is how surface/subsurface oxygen in CuO_x improves the selectivity towards C_2 products (as compared to pure Cu). As the electronic structure of such oxide-derived copper is different from pure Cu, it should play an important role in the reaction selectivity. ARPES studies showed that for Cu(001) oxygen adsorbates induce surface states near the Fermi energy [18]. However, it is unclear how these states evolve when oxygen is introduced into the subsurface. Moreover, the new electronic states could be rather exotic, as in the case of Dirac fermions emerging in the layer of adsorbed CO on Cu(111) [19]. Similar adsorption-induced modification of the electronic structure, including Fermi surface reconstruction and changes in the surface potential, occur on other metals [20].

The examples above describe the use of ARPES for understanding the adsorption of molecules on surfaces. Currently, there are no general predictors for the evolution of the Fermi surface, electronic bands and their dispersion during adsorption. A fair accuracy in theoretical predictions of ARPES data can be achieved by using density function theory and dynamical mean-field theory [21]. When it comes to electrochemical interfaces, the processes are further complicated by the presence of the electrical double layer and solvent. Despite the advances in *ab initio* molecular dynamics simulations [22–24], the description of the double layer is still far from being quantitatively predictable [25,26]. The theoretical frameworks for the electrochemical charge transfer based on model Hamiltonians (such as Santos-Koper-Schmickler model [27,28], which is based on the Anderson-Newns model for chemisorption) incorporate densities of states as a parameter but not the dispersion of bands or other nuances of the electronic structure. Thus, the role of the Fermi surface and band dispersion in electrocatalysis is currently unclear. ARPES experiments can provide more detailed information on the role of electronic structure in adsorption and electrochemical reactions compared to traditional X-ray photoelectron spectroscopy and X-ray absorption spectroscopy. In the field of gas-phase catalysis and liquid electrochemistry, X-ray photoelectron spectroscopy at near-ambient pressures (NAP-XPS) is used for *in situ* studies of surfaces (e.g. 'dip-and-pull' method) [29]. However, NAP-XPS cannot be employed in the *in situ* 'ARPES' mode because the detected signal is too weak to provide meaningful angle-resolved datasets. Performing *in situ* ARPES with a gas or liquid present in the analytical chamber is currently impossible.

Here, we discuss alternative ways to link ARPES data to the electrochemical response of a surface: (1) by probing the difference in ARPES maps between pristine and adsorbate-covered surfaces (where adsorbates are relevant to the catalytic reaction); (2) by using a series of surfaces with a systematically varying composition where the trends in ARPES results can be compared to the trends in electrochemical behavior; (3) by performing ARPES on a surface that undergoes electrochemically induced transformations (i.e. changes in photoemission spectra can be correlated to structural and chemical changes at the surface). Using oxide surfaces as an example, we explore how ARPES can be integrated with electrochemistry and identify relevant experimental challenges.

3. ARPES and the electrochemical response of perovskite oxides

Perovskite oxides have remarkably diverse electronic properties, which results in composition-dependent electrochemical response, electrocatalytic activity and photoemission spectra. Typical perovskites such as $SrTiO_3$ or $LaNiO_3$ have a Fermi surface that originates predominantly from the transition metal states [30]. ARPES measurements of such perovskites reveal various phenomena such as 2D electron gas [31] that depends on the surface reconstruction [32], Fröhlich polarons [33], nodal structures in spin-polarized bands [34], thickness-dependent quasiparticle behavior (metal-insulator transition) [35], and others. The extent of ARPES literature for perovskites is vast, making such materials ideal candidates for bridging ARPES with electrochemical experiments.

However, the major challenge with perovskites (and oxides in general) is that achieving and maintaining a high surface quality is difficult. As we described previously in a review [2], oxides can exhibit complex surface restructuring that changes their electronic and electrochemical properties. Because the near-surface region determines the electrochemical response and intrinsic electrocatalytic activity, it is challenging to measure precise electrochemical quantities (activity, redox peaks, intercalative currents). The problem is further exacerbated by the structural and chemical evolution of the near-surface layer under electrochemical conditions (cation leaching, oxygen insertion/de-insertion, transition metal dissolution). This fact necessitates the use of well-defined (single-crystalline) oxide surfaces for the precise electrochemical and ARPES measurements.

The electrochemical response of the ABO_3 perovskites strongly depends on the transition metal, while the structural stability largely depends on the leaching rate of the A-cation and the solubility of the transition meta [2,36–39]. When A-cations leach out, the perovskite structure can collapse into an amorphous state [37,38] that exhibits higher currents in the pre-OER region than a single-crystalline surface, which is likely associated with ion insertion/de-insertion reaction (e.g. O^{2-} or electrolyte cations) and has contributions from surface adsorption and the double layer. Redox peaks are not always pronounced in

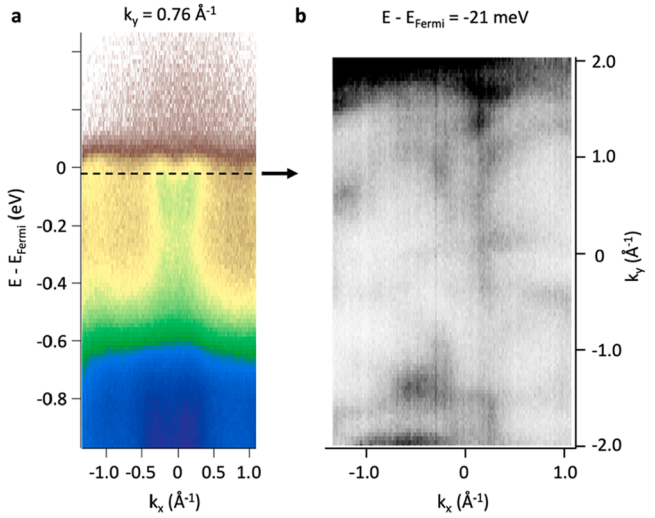

Fig. 1. ARPES measurements of the (001) $LaNiO_3$ after surface restoration by heating. (a) Momentum distribution map at k_y=0.76 Å^{-1}. The band dispersion (V-shaped curve) is visible near the Fermi level and is symmetric with respect to k_x. (b) The Fermi surface become visible for the $LaNiO_3$ surface after the sample was heated *in situ* (inside the ARPES setup) at 700 °C and $pO_2 = 10^{-6}$ mbar for 10 min. The Fermi surface is plotted in the k_x-k_y plane of the reciprocal space by taking a cut at −21 meV below the Fermi level.

perovskites, the reason for which is not well understood (although the preparation procedure and surface restructuring could be a contributing factor [40]). As we mentioned above, due to intrinsic instability of many perovskites under OER and ORR conditions, the electrocatalytic currents are hard to record for a perfect perovskite surface (for which the adsorption energies are typically calculated via density functional theory). Thus, the currently reported trends in the OER and ORR activities on perovskites are questionable.

4. Transfer of electrocatalytic oxide material to an ARPES chamber and surface restoration

To avoid contamination or remove it after air exposure, the following is commonly used in the ARPES experiments that are performed off-site at specialized labs and synchrotron beamlines:

(a) A vacuum suitcase for transferring the sample from the preparation chamber to a beamline. The vacuum suitcase is a small, often tubular 'chamber' with samples inside and an active pump (e.g., getter-based). Such UHV suitcases can be shipped to a synchrotron by air. The downside is that it is a UHV-to-UHV solution and cannot incorporate wet electrochemistry.
(b) Cleaning an air-exposed surface by ion bombardment (sputtering) inside a separate "preparation" chamber at a beamline. Because it induces surface changes, this approach works well for surfaces that can be restored in UHV with heating such as metals. Unfortunately, oxide materials lose oxygen upon sputtering and cannot be restored by annealing without sufficiently high temperatures and pO_2.
(c) Removal of contaminants by heating up the sample in UHV and inducing desorption of molecules from the surface. As with sputtering, this method can change the surface. For oxides, it works well only when (1) pO_2 in the chamber is high enough for the near-surface region to maintain its oxygen stoichiometry and (2) surface restructuring is not observed after the procedure.

In our experiments, we use epitaxial (001) $LaNiO_3$ and (001) $LaFeO_3$ films (10 unit cells thick) as model electrocatalysts. The films were grown with pulsed laser deposition (PLD) on Nb-doped $SrTiO_3$ substrates at 625 °C (see Methods). The samples were exposed to the environments typically used in electrochemical experiments (air and N_2-filled glovebox) with the aim to evaluate its effect on the quality of ARPES measurements.

To restore the surface of air-exposed $LaNiO_3$ and $LaFeO_3$ films, we first performed annealing inside the preparation chamber at the ARPES beamline (1ˆ2 beamline at BESSY, Germany [41]). We start with lower temperatures to minimize the effect of annealing. At each step, $LaNiO_3$ was heated to increasingly higher temperatures: 360 °C (20 min), 500 °C (15 min), 650 °C (20 min), and 700 °C (10 min) at $pO_2 = 10^{-6}$ mbar. For $LaFeO_3$, we used temperatures up to 800 °C (9 min). After each annealing, the sample was transferred *in situ* (UHV) to the ARPES chamber for photoemission measurements (see Methods). We found that the band dispersion for $LaNiO_3$ becomes visible only after annealing at 700 °C (Fig. 1), which is likely due to CO_2 desorption. However, the Fermi surface only remotely resembles the one reported previously for *in situ* transferred $LaNiO_3$ [35,42]. The most likely explanations are (1) the residual carbonaceous specie at the surface, (2) changes in the surface composition or (3) excessive oxygen loss (reduction under 10^{-6} mbar of O_2) that make it hard to measure the Fermi surface. In such cases, if the ARPES beamline can work soft X-rays near the absorption edges relevant to the surface, core-level spectroscopy can help to understand the reason for poor ARPES signal (not all ARPES beamlines are designed to work with the full range of soft X-rays). For $LaFeO_3$, no band dispersion or clear Fermi level was observed up to 800 °C. Because this exceeds the growth temperature by 175 °C, we suppose that either certain surface adsorbates are too strongly bound to the surface or the $LaFeO_3$ phase decomposed at the surface.

These results indicate the following:

(a) Adsorbates from air exposure may require high temperatures to be removed (close to or above the synthesis temperature).
(b) Different oxides require different annealing conditions.
(c) Oxygen loss during annealing in low pO_2 can lead to changes in the Fermi surface. To address it, one can follow a two-step process: first, bake the sample at high temperatures under low pO_2 to induce desorption, and then anneal the sample at a lower temperature but higher pO_2 (e.g., 0.1–100 mbar, depending on the oxide surface). Alternatively, if desorption requires concurrent oxidation of surface molecules, it can be done directly under high oxygen pressure. Currently, the problem is that a high pO_2 can be achieved only in a separate non-UHV chamber that is often unavailable at beamlines.

Here we should also highlight that perovskites can have variable termination that depends on the preparation conditions (T, pO_2) [40]. This can further complicate the surface restoration before ARPES experiments.

5. Surface contamination after electrochemical tests

Oxide electrocatalysts work well for oxygen evolution and reduction reactions (among others). During oxygen evolution (water oxidation), the surface is brought out of thermodynamic equilibrium and can change its chemical composition and structure. For example, an oxide material can experience cation leaching (de-intercalation) [43,44], OH^- intercalation [45], loss of lattice oxygen [46–49], partial amorphization [38,50], and/or transition metal dissolution [1,51], as well as the precipitation of trace impurities from the electrolyte [52,53]. However, little is known about the evolution of the electronic structure during such transformations and how it is linked to the altered electrochemical response and electrocatalytic activity. By probing the electronic properties of an oxide surface as it evolves from an ideal (model) into a real (operating) state, we can learn how the disruption of the crystal lattice at the surface modifies its electronic structure and electrocatalytic activity.

However, photoemission studies of surfaces that underwent

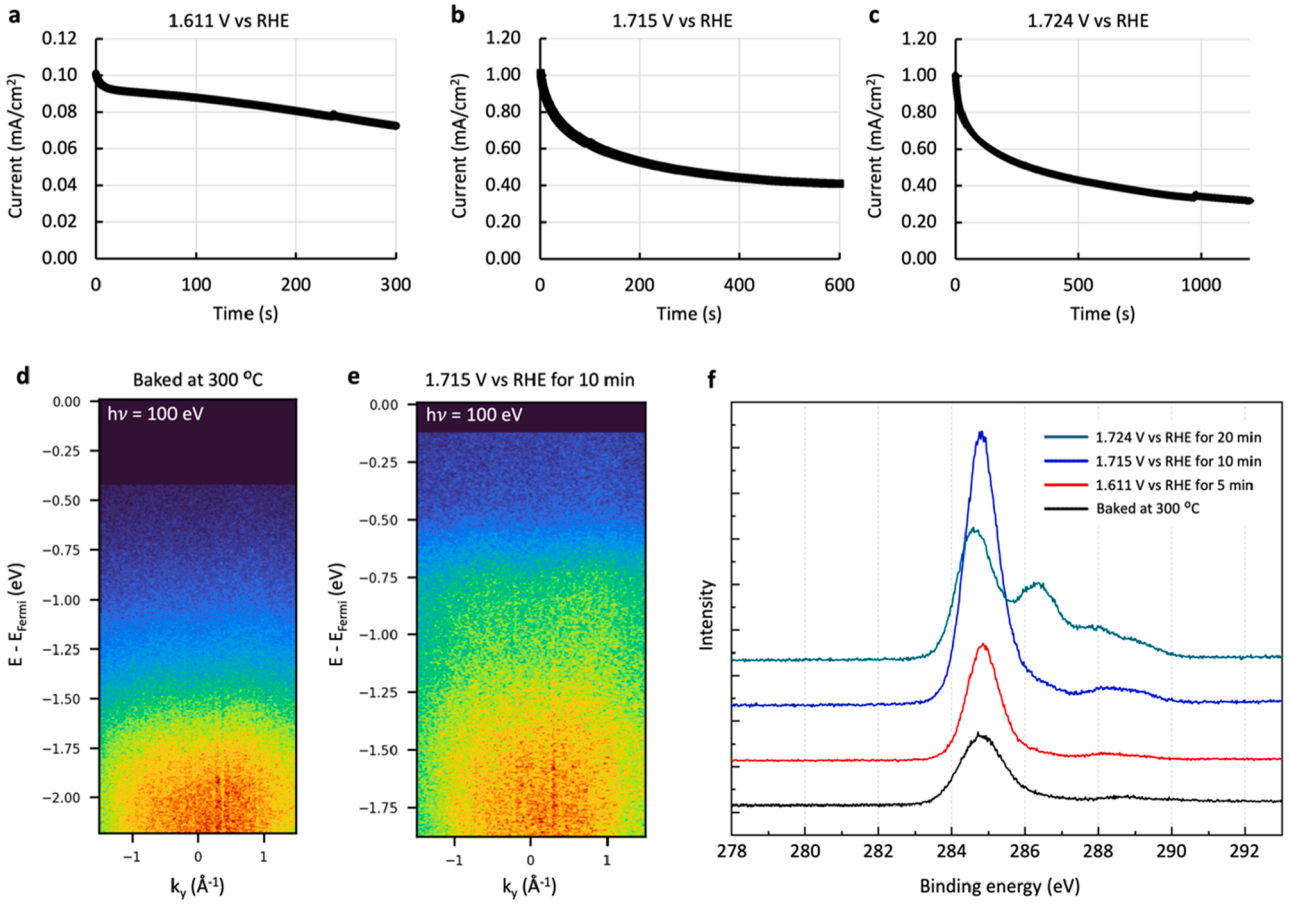

Fig. 2. (a-c) Chronoamperometric curves recorded for the same (001) $LaNiO_3$ surface at different potentials (each measurement was followed by an ARPES experiment). (d-e) Momentum distribution maps for the $LaNiO_3$ surface after (d) being heated at 300 °C and $pO_2 = 10^{-6}$ mbar for 30 min and (e) chronoamperometry at 1.715 V vs RHE for 10 mins. The maps show integrated intensity along k_x between (a) 0.00–0.01 $Å^{-1}$ and (b) 0.00–0.05 $Å^{-1}$. (f) Carbon 1 *s* XPS for the sample shown in (a) and (b) after different treatments. XPS reveals carbonaceous specie are still present at the surface. The electrochemical tests were conducted in an N_2-filled glovebox, and the samples were transferred to the beamline in a UHV suitcase without air exposure. These experiments show that the electrolyte or/and the glovebox environment are the source of surface contamination and are not suitable for combining ARPES with wet electrochemistry.

electrochemical tests are challenging. The key difficulty is to preserve the surface after an electrochemical experiment and avoid its contamination. Generally, contaminants come from: (1) the solvent that can leave adsorbed molecules on the surface; (2) dissolved salts that can have contaminating specie such as carbonates, sulfates, chlorides, and others; (3) gas environment after the sample is taken out of a cell. The electrochemically evolved surface should be measured "as-is" because it can have very delicate atomic structure that cannot be thermally treated to induce desorption of contaminants. As a result, a few potential ways to preserve it for ARPES include:

(a) Performing electrochemical tests in a special glovebox to minimize air exposure and then transfer the sample to a UHV chamber using a special UHV-to-glovebox suitcase. This approach is easy to implement and requires minimal resources and was used for conventional X-ray photoelectron spectroscopy (XPS) before [54]. However, such a glovebox may not have sufficient purity of the environment for ARPES.

(b) Building a separate UHV chamber where electrochemistry can be performed after filling it up with ultrapure inert gas. In this case, electrolytes should be prepared inside the chamber using UHV-compatible syringes and ultrapure salt (e.g. NaCl or SrO single crystals) to avoid any extrinsic contamination. Substantial resources are required for setting up and operating such a chamber. Importantly, it should be available next to a synchrotron source to minimize the sample transfer time. The description of such a chamber is provided below.

Here we attempt to minimize the surface contamination after electrochemical tests by employing a separate custom-made N_2-filled glovebox. Potentiostatic tests were performed on $LaNiO_3$ films in 0.2M KOH. After each test, the sample was first flushed five times with ultrapure water and then placed into a vacuum suitcase connected to the glovebox. This suitcase was then sealed and reconnected to a UHV chamber at the beamline and pumped down. Fig. 2 shows energy dispersion maps measured after baking the sample at 300 °C and a chronoamperometric test at 1.715 V vs RHE for 10 mins. In these experiments, we do not see a clear Fermi level and band dispersions. X-ray photoelectron spectroscopy (XPS) shows the presence of surface adsorbates (carbonaceous specie) that most likely make bands poorly visible. The oxygen evolution reaction represents a strongly oxidizing condition at the surface and should oxidize most carbonaceous specie to CO_2. Since we do not see any improvement in ARPES maps when water oxidizing potentials are applied, we suggest that either (1) adsorbates stay intact during water oxidation or "re-contaminate" the surface from the electrolyte after the potential is back to the open circuit (KOH always has K_2CO_3 impurities) or/and (2) the environment inside the glovebox itself contains sufficient concentration of impurities to contaminate the surface. This is not surprising because maintaining the gas purity inside the glovebox below ~ 1 ppm is difficult. 1 ppm would correspond to a partial pressure of 10^{-3} mbar, which is beyond the typical range of UHV

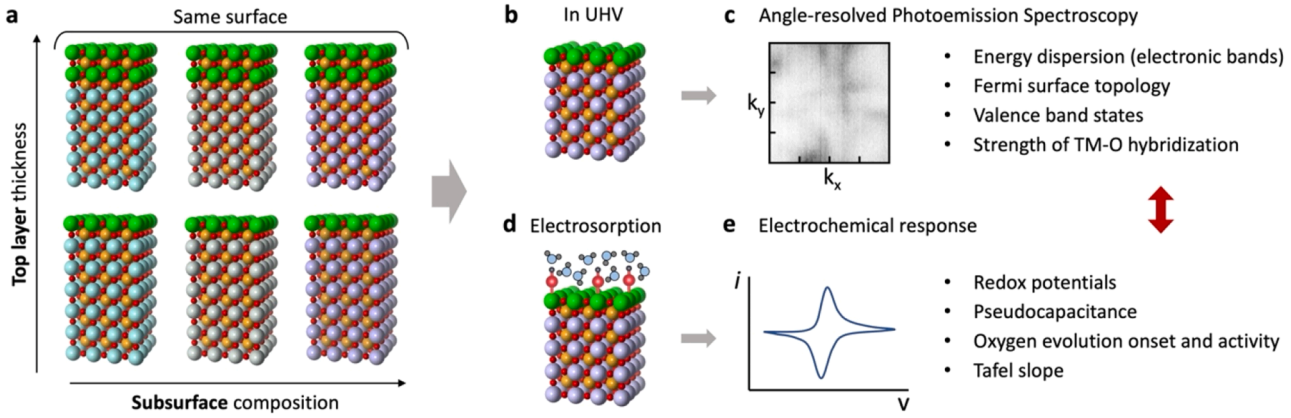

Fig. 3. (a) The concept of subsurface tunability of adsorption strength in perovskite oxides using an atomically precise growth of heterostructures. (b) Correlation of the surface electronic structure and electrochemical response.

ARPES. Essentially, our experiments show that avoiding surface contamination in a glovebox can be too challenging, despite its common use in electrochemical experiments that should avoid air exposure (e.g. batteries [55]) or require high-purity environment [54]. Ideally, for such studies one should construct a UHV chamber that is compatible with electrochemical experiments that employ ultrapure chemicals and gas (ideally, below 1 ppb).

6. How to reduce the effect of contaminants in ARPES

In addition to the transfer of samples in vacuum (directly or in a UHV suitcase), one can consider the following approaches:

Resonant ARPES. By tuning the incident X-ray energy to the absorption edges of elements, one can resonantly enhance the spectral weight in ARPES [56–60]. Significant enhancement can be expected for the localized states in the participating conduction or valence bands [61, 62]. With resonant ARPES, it is possible to reveal element-specific contribution (TM and O) to the electronic band structure and Fermi surface. For example, previous studies of the $LaAlO_3/SrTiO_3$ interface show individual contributions from Ti^{3+} and Ti^{4+} in resonant ARPES spectra [57]. Moreover, the resonant enhancement allows for measuring the spectral features of elements in very small concentrations (e.g., Mn states at 2.5 at.% in $Ga_{0.975}Mn_{0.025}As$ [60]).

Subsurface ARPES. When ARPES is performed using photon energies close to 1 keV, the probing depth can be improved dramatically compared to ultraviolet ARPES. In the previous work [61], Strocov et al. provides examples of probing buried quantum wells and impurity using photons with a high kinetic energy. The key drawbacks of this approach are a low photoexcitation cross-section and increased phonon excitation.

Hard-X-ray ARPES (HARPES). This technique can probe the subsurface and bulk of a material, which is especially valuable when analyzing the evolution of the electronic structure after an electrocatalytic reaction. Despite certain challenges [63,64], this method can be an alternative to regular soft X-ray ARPES. It employs high kinetic energies of electrons and can probe the electronic structure at the depth of over 5 nm, revealing the difference between the bulk electronic structure (that defines the physical properties of oxides) and the surface (which defines electrochemical adsorption) [65–67]. Similarly to the case of subsurface ARPES, this approach is hindered by an increasingly lower cross-section for valence-band photoexcitation and a lack of coherent spectral weight [61].

7. Future perspective

Electronic band structure of the near-surface layer can be very complex [68], and its experimental analysis requires a careful study of the Fermi surface, electronic band dispersion, contribution of individual elements to the density of states in the valence band, and other parameters. While these parameters may influence the kinetics of charge transfer, their connection to electrochemical adsorption and electrocatalysis remains unclear. In this regard, one can ask relevant fundamental questions such as:

1. To what extent does the Fermi surface and its change upon adsorption determine the adsorption strength and electrochemical response of a surface?
2. How does the band dispersion (*k*-vector dependence of the electron energy) affect the electron transfer during adsorption and electrochemical transformations of the molecules? Does it correlate with theoretical predictions?
3. What is the role of the metal-ligand hybridized states in the stabilization of intermediates (e.g. Co-O states in oxygen evolution, or Cu-O states in CO_2 reduction on a copper oxide)?
4. How does the distribution of the density of states in the valence band affect the electrocatalytic reaction rate?
5. How does the electronic structure evolve under electrochemical conditions?

To experimentally address these questions, creative solutions are needed to bridge the gap between UHV ARPES and electrochemical experiments. Below, we describe some possible pathways that could help an interested experimentalist to come up with great approaches and solutions.

7.1. ARPES of atomically defined heterostructures

By carefully separating surface from the bulk, one can explore the relationship between the finely tuned electronic structure and electrochemical response. Using modern growth methods (molecular beam epitaxy, pulsed laser deposition or sputtering), it is possible to synthesize single-crystalline oxides in the form of epitaxial films with atomic precision. Fig. 3 shows single-crystalline surfaces that have the same surface composition but different subsurface chemistry. Previously, similar surfaces were studied as electrocatalysts by Akbashev et al. [1] for the oxygen evolution and Eom et al. for the oxygen reduction reaction. In the epitaxial growth, different unit-cell-thick layers can be “added” on top of each other (epitaxy thermodynamically stabilizes the system) as long as their crystal structure is not too complex (large unit cells, multi-elemental doping, etc.). By controlling the exact chemistry within the near-surface layer, one can tune (1) its electronic properties via electron/hole donation from the subsurface [1] and (2) the orbitals at the surface that can bind to adsorbates and participate in electrocatalysis. Such atomically defined heterostructures can reveal the

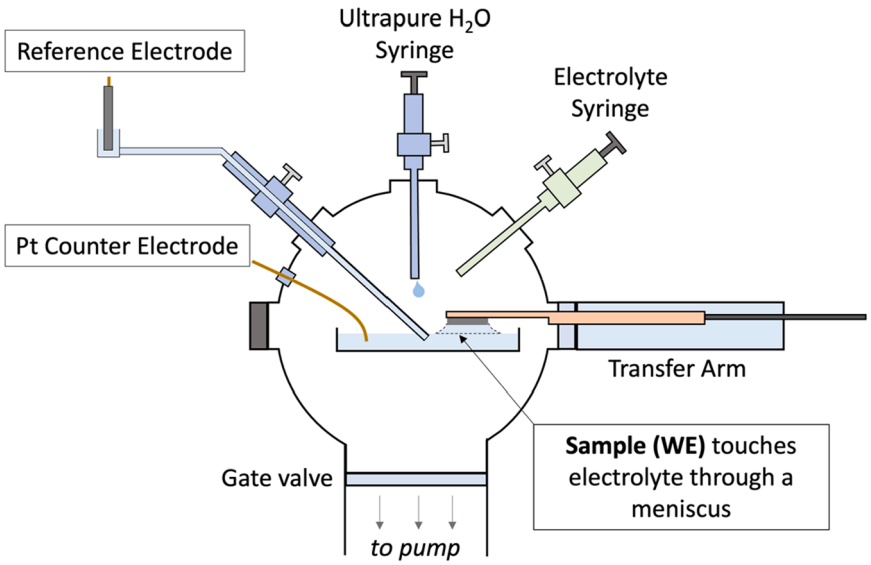

Fig. 4. Electrochemistry-compatible UHV chamber for preserving the samples from air exposure and surface contamination.

correlations between the adsorption-induced electronic structure, surface/subsurface chemistry and the electrochemical response (electrosorption and redox behavior, pseudocapacitive response, electrocatalytic activity, Tafel slope).

Importantly, ARPES experiments can be extended to studying adsorption-induced changes in the valence band structure and Fermi surface. For example, when exposed to molecules such as H_2O, D_2O, H_2O_2 or atomic oxygen in a preparation chamber (most ARPES beamlines have such capabilities), the oxide surface can undergo hydroxylation or peroxidation [69,70] and experience an electron transfer that is reminiscent of what happens during electrosorption and certain electrocatalytic reactions. The electron transfer during such adsorption of the surface [12,14,71,72]. Although the system lacks an electrochemical interface, the trends in chemisorption on various surfaces may still provide insight that is relevant to electrochemical reactions. Once transferred to the ARPES chamber, the sample should stay at temperatures where no desorption occurs under UHV and X-ray radiation. As a result, one can gain further insight into the relationship between the surface/subsurface chemistry and charge transfer processes.

7.2. Probing the evolution of electronic structure of the surface via ARPES

Electrocatalytic conditions can introduce compositional changes and structural rearrangement in materials. Any change in the near-surface layer can have a profound impact on the charge transfer kinetics and electrochemical response. As already mentioned previously, such transformations can include alkali-earth cation leaching [43,44] from oxides, amorphization [38,50,73], dissolution and precipitation reactions [36], and others. Cation leaching (deintercalation) results in open sites inside the crystal lattice that can either (1) accommodate anionic species (e.g., OH^- intercalated during OER [45]) or foreign cations (Li^+, Na^+, K^+ or H^+). It can significantly modify the electronic structure of the near-surface region. Ultimately, when the concentration of defects in the near-surface becomes high, a structural collapse and partial disorder can take place. Although some amorphous materials can show dispersive bands [74], ARPES of disordered surfaces normally shows no momentum-dependent features.

Quantitative analysis of the surface evolution requires a single-crystalline material as a starting (reference) point on the “evolution axis”. Obviously, cleaning and preserving the surface after each electrochemical experiment presents a major challenge. As our experiments show, a dedicated glovebox cannot provide the required atmospheric purity. To avoid surface contamination (to which ARPES is exceptionally sensitive), an electrochemical setup integrated with a UHV chamber should be built. In between electrochemical experiments, the chamber is maintained under UHV. For an electrochemical experiment, it is filled with ultrapure argon that passes through CO_2 and hydrocarbons traps (the gas purity can be below ppb, reaching lower ppt levels with appropriate purification). Fig. 4 shows the basic components: an externally controlled syringe for the electrolyte delivery/removal (valves are closed during evacuation). An additional syringe is used for a reference electrode that is connected externally through the fluidic line filled with an electrolyte (if the impedance of the fluidic line is high, a Pt shunt can be connected to the reference line through a capacitor to remove high-frequency artifacts [75]). An externally connected reference was used before by Akbashev et al. in electrochemical atomic force microscopy and allowed to minimize the number of components immersed into the cell. In the case of a UHV chamber, an external reference can be disconnected by simply closing the valve during evacuation and then connected into the 3-electrode configuration after the chamber is filled with an inert ultrapure gas. Pt wire is used as a counter electrode. An additional syringe for flushing the sample with ultrapure water will be needed as well. The electrolyte container can be made of Teflon since it is vacuum-compatible. The sample is connected to the holder on a transfer arm and can touch the electrolyte either through immersion or by forming a hanging meniscus. After the experiment is finished and the electrolyte is removed, the surface is flushed with ultrapure water, and the chamber can be pumped down to UHV again. Importantly, electrolytes should be as free as possible from carbonates and other impurities.

The chamber should be either connected to a UHV suitcase or directly to the ARPES beamline. During the ARPES measurements in between the electrochemical tests, the sample can be cooled down to minimize possible X-ray damage. In consecutive experiments, the changes of the Fermi surface, the density of transition metal (TM) and oxygen states in the valence band, and the degree of TM-O hybridization can be monitored as a function of structural reconstruction. The reconstruction itself can be probed, for example, via photoelectron diffraction (at soft X-ray ARPES beamlines) or surface X-ray scattering (separate experiments). At some ARPES beamlines (such as PEARL at Swiss Light Source [76]), it is also possible to perform XPS to probe chemical composition and oxidation state of the elements in the near-surface region.

The electrochemical response of single-crystalline surfaces can be studied via a potential-dependent electrochemical impedance spectroscopy (in addition to the traditional cyclic voltammetry). It allows for the derivation of the charge transfer resistances, pseudo- and double-layer

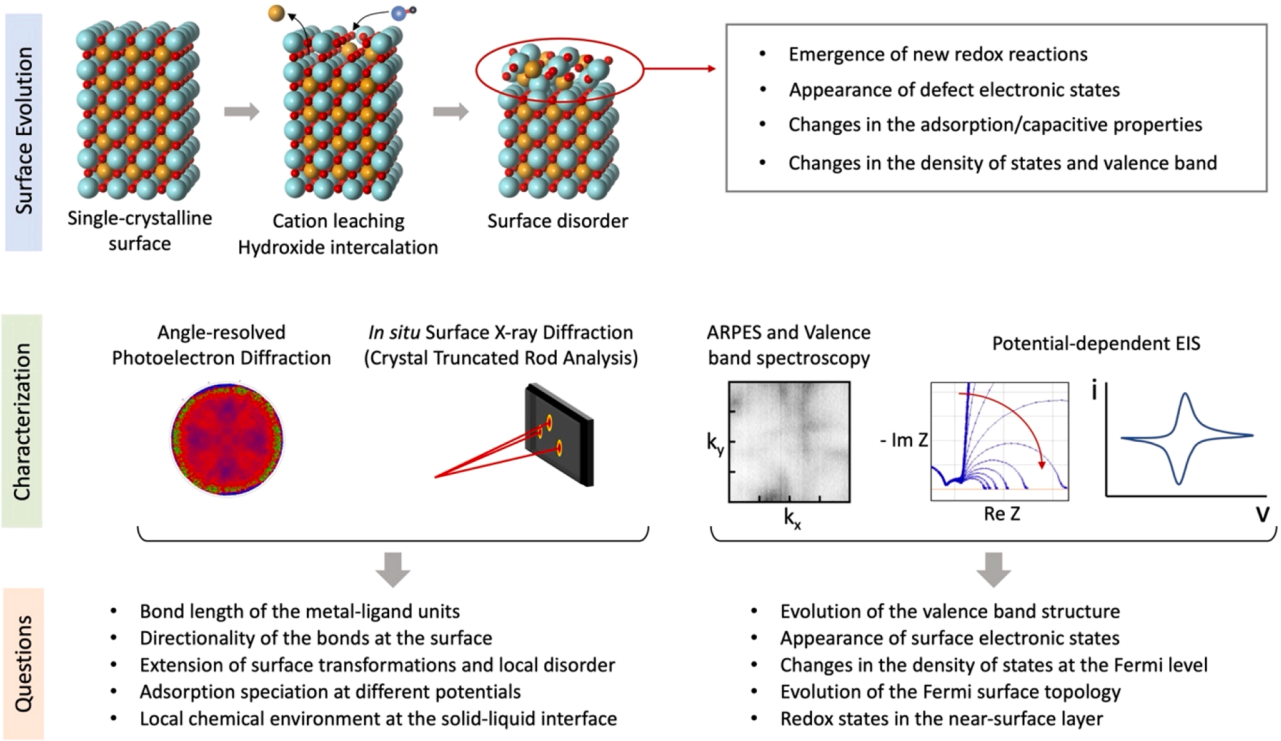

Fig. 5. Restructuring and degradation of single-crystalline perovskite surfaces during OER. Sophisticated characterization is required to track the gradual evolution of electronic and atomic structure of the surface as well as its morphology and electronic conductivity. EIS – electrochemical impedance spectroscopy.

capacitances at different stages of the surface evolution (when it is slow enough compared to the timescale of one impedance spectrum). *In situ* amorphized surface oxide layers often exhibit higher capacitive currents that can be associated with the intercalative processes similar to the well-known pseudocapacitance observed in hydrous ruthenium oxides [77]. With a careful fitting, one can study subsurface ion diffusion by including into the circuit analysis the circuit element for the finite-length Warburg impedance associated with the ion diffusion in solids [77,78].

Studies of precipitates. Electrocatalytic processes are highly sensitive to minor variations in the electronic and atomic structure of a near-surface layer. Fe (oxy)hydroxide precipitation from sub-ppm trace amounts in an electrolyte have been found to induce considerable increase of electrocatalytic activity [52,53,79]. How exactly such (nanoscale) precipitates affect the electronic structure of the surface remains unknown. Using ARPES, one can probe the changes in the electronic structure during precipitation of Fe^{3+} from the trace impurities in the electrolyte.

7.3. Combining ARPES with other techniques

As high-quality ARPES can be done only *ex situ*, one should consider combining it with *in situ* spectroscopic or diffraction techniques. For example, surface X-ray diffraction is the only X-ray scattering technique that can be performed *in situ* under electrochemical conditions and has a high sensitivity to the molecular and crystal structure at the interface [80–84]. Traditional surface diffraction involves collection of crystal truncation rods (CTR) using a grazing-incident X-ray beam with an emphasis on the anti-Bragg regions of the CTR. It can provide information about the electrosorbed cations (the Stern layer [81]), coordination of water molecules [81] around the interfacial cations and an insight into the electrical double layer [82]. Moreover, surface diffraction can reveal the adsorption-induced lattice relaxation of the surface in different electrolytes [82], which is vital for understanding surface restructuring and degradation. This makes *in situ* surface X-ray scattering and ARPES an ideal combination for correlating the electrochemical adsorption and detailed electronic structure for electrocatalysts.

An example of a subsurface-tunable system that can be probed by *in situ* CTR and *ex situ* ARPES / XPS is shown in Fig. 6. The surface AMO_3 layer covers a range of transition metals (Cr^{3+}, Mn^{3+}, Fe^{3+}, Co^{3+}, Ni^{3+}, Ir^{4+}, etc.) that have *d*-level occupancies changing from low to high. The subsurface layer can $LaNiO_3$ or (La,Sr)MnO_3 as they provide sufficient electronic conductivity. This system should span a range of adsorption energies and can be studied with combined surface diffraction and ARPES.

Another important technique to probe the surface/subsurface structure is photoelectron diffraction and holography. It involves diffraction of photoelectrons on the neighboring atoms and provides element-specific information about the local atomic structure within a thin surface layer. Photoelectron diffraction requires oriented local structures but not long-range translational symmetry (unlike for X-ray diffraction). Therefore, it can probe partially disordered systems such as intercalated materials, dopant sites and adsorbate-covered surfaces [85]. The measurements can be performed by detecting photoelectrons [86–89] or Auger electrons [90]. Previously, the technique was also used for the surfaces of binary oxides [91] and perovskites [92,93]. With the probing depth of 1–3 nm, photoelectron diffraction is ideal for the analysis of the surface transformations in single-crystalline samples [94], especially in the early stage when the surface is only partially disordered. Recently developed reconstruction algorithms [95–97] for the photoelectron holography enable the accuracy of ~ 0.1 Å in the reconstructed atomic positions in the surface and subsurface regions. Some ARPES beamlines can be used to collect the photoelectron diffraction (for example, PEARL beamline at SLS [76]), making it possible to combine these analytical approaches in the same experiment.

Finally, it is important to combine ARPES with *in situ* X-ray photoelectron and X-ray absorption spectroscopies whenever possible. First, 'dip-and-pull' XPS [98] can give information about the redox state of surface transition metals in the potential range where mass transport can

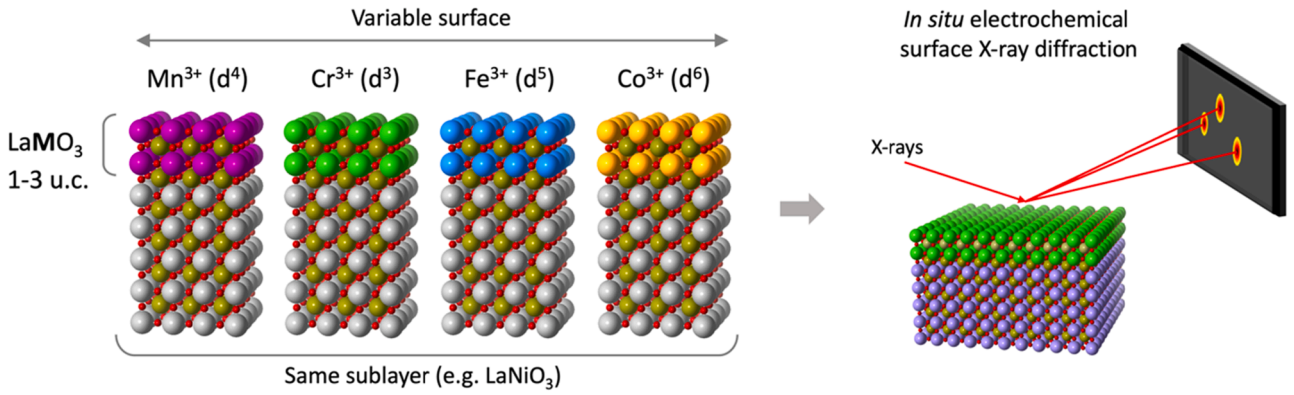

Fig. 6. Electrocatalytic surfaces with different *d*-level filling at the surface.

be neglected (i.e. pseudocapacitive, surface redox and the double layer regions). Although the 'dip-and-pull' method is commonly used for solid/electrolyte interfaces these days, one has to be careful with the drawbacks and artifacts that could arise in such experiments [99]. Second, grazing-incidence hard X-ray absorption spectroscopy [100] (K-edge) can help understand the intercalative phenomena in the near-surface region. However, as hard X-ray absorption does not have a high scattering cross-section, it may be challenging to probe the near-surface layers for certain elements (such as Fe).

8. Conclusion

Bridging the gap between high-quality ARPES measurements and electrochemical experiments is exceptionally difficult. Here, we discussed the challenges and possible solutions for oxide electrocatalysts. Our experiments show that the combination of a glovebox and vacuum suitcase that allows for successful XPS measurements of the surface does not imply that dispersion curves and Fermi surface would be distinguishable in ARPES. Carbonaceous specie cannot be easily removed by annealing the sample without disturbing the surface. We anticipate that special annealing chambers with high pO_2 capabilities (10^{-3} to 1 mbar) are needed for restoring the oxide surfaces that were exposed to air. We also suggest that a UHV chamber compatible with wet electrochemistry can become an important step toward enabling ARPES on electrocatalysts. However, care should be taken in purifying solvents and salts, as these are the main sources of surface contamination. Unfortunately, most conventional electrolytes are based on salts such as KOH or $NaClO_4$ and contain carbonate impurities that are hard to remove.

Ultimately, we discuss how atomically precise oxide heterostructures can be used in ARPES and surface X-ray scattering. Such correlative experiments can provide long-sought insights into the detailed electronic properties of the surface relate to the potential-dependent electrosorption during electrochemical reactions and electrocatalysis (Fig. 5).

Declaration of competing interest

The authors declare that they have no known competing financial interests or personal relationships that could have appeared to influence the work reported in this paper.

Methods

The thin films were grown on Nb-doped (0.5 wt%) $SrTiO_3$ (100) substrates (Shinkosha Co.) using a 248 nm KrF excimer laser (COMPexPro, Coherent) operated at 1 Hz with the laser fluence of 1.6 mJ/cm^2. The growth was monitored using reflective high-energy electron diffraction (RHEED) to ensure the films grow in a two-dimensional mode and the surface has a high crystalline quality. First, a 1-u.c. $LaTiO_3$ layer was grown ($pO_2 = 1.2 \times 10^{-3}$ mbar) to reduce the space charge in Nb-doped $SrTiO_3$ and ensure a better conductivity through the interface [101]. $LaNiO_3$ and $LaFeO_3$ were grown at 625 °C at $pO_2 = 23\times10^{-3}$ mbar. For the $LaFeO_3$ samples, a sublayer of 10 u.c. $LaNiO_3$ was added for better conductivity. For electrochemical measurements, electrical contacts were sputtered on the back of the Nb-doped $SrTiO_3$ substrates.

Electrochemical experiments were carried out using a rotating disk electrode customized for epitaxial films in 0.2 M KOH. The electrolyte was purified from traces of Fe by running an anodic current of 1 mA through a nickel wire (99.999 %, ThermoFisher Scientific) for at least 24 h (similarly to the procedure described previously [53]). All measurements were performed in a three-electrode setup with a Hg/HgO reference electrode (1M KOH, CH Instruments) and a Pt mesh counter electrode (99.9 %, Sigma-Aldrich) using the SP-300 potentiostat (Biologic).

ARPES experiments were performed at two beamlines: the PEARL beamline (Swiss Light Source) and the 1^2 beamline (BESSY II). Samples were cooled down to 90–100 K during the measurements. Prior to each ARPES measurement at PEARL, the sample was tested electrochemically in a small N_2-filled glovebox and transferred to the ARPES chamber using a UHV suitcase.

Acknowledgements

The authors acknowledge Paul Scherrer Institute (Villigen, Switzerland) for provision of synchrotron radiation beamtime at beamline PEARL - X03DA of the SLS. The authors are also thankful for ARPES One-Square instrument at U112-PGM-2a-12 beamline at the BESSY II electron storage ring operated by the Helmholtz-Zentrum Berlin für Materialien und Energie.

References

[1] A.R. Akbashev, et al., Activation of ultrathin $SrTiO_3$ with subsurface $SrRuO_3$ for the oxygen evolution reaction, Energy Environ. Sci. 11 (2018) 1762–1769.
[2] A.R. Akbashev, Electrocatalysis on oxide surfaces: fundamental challenges and opportunities, Current Opin. Electrochem. 35 (2022) 101095.
[3] W. Schmickler, E. Santos, Interfacial Electrochemistry, Springer Science & Business Media, 2010.
[4] C.J. Eom, et al., Tailoring manganese oxide with atomic precision to increase surface site availability for oxygen reduction catalysis, Nat. Commun. 9 (2018) 4034.
[5] H. Yang, et al., Visualizing electronic structures of quantum materials by angle-resolved photoemission spectroscopy, Nature Rev. Mater. 3 (2018) 341–353.
[6] B. Lv, T. Qian, H. Ding, Angle-resolved photoemission spectroscopy and its application to topological materials, Nature Rev. Phys. 1 (2019) 609–626.
[7] J.A. Sobota, Y. He, Z.-X. Shen, Angle-resolved photoemission studies of quantum materials, Rev. Mod. Phys. 93 (2021) 025006.
[8] S. Hüfner, Photoelectron Spectroscopy: Principles and Applications, Springer Science & Business Media, 2013.
[9] R. Gomer, Approaches to the theory of chemisorption, Acc. Chem. Res. 8 (1975) 420–427.

[10] J. Ziroff, F. Forster, A. Schöll, P. Puschnig, F. Reinert, Hybridization of organic molecular orbitals with substrate states at interfaces: PTCDA on silver, Phys. Rev. Lett. 104 (2010) 233004.
[11] H.-G. Boyen, et al., Local density of states effects at the metal-molecule interfaces in a molecular device, Nat. Mater. 5 (2006) 394–399.
[12] M. Wießner, et al., Substrate-mediated band-dispersion of adsorbate molecular states, Nat. Commun. 4 (2013) 1514.
[13] H. Mizushima, et al., Effect of physisorption of inert organic molecules on Au (111) surface electronic states, Phys. Chem. Chem. Phys. 19 (2017) 18646–18651.
[14] Y.S. Kim, et al., Role of preferential weak hybridization between the surface-state of a metal and the oxygen atom in the chemical adsorption mechanism, Phys. Chem. Chem. Phys. 15 (2013) 19019–19023.
[15] Y.S. Kim, et al., Role of transition metal in fast oxidation reaction on the Pt3TM (111) (TM = Ni, Co) surfaces, Adv. Energy Mater. 3 (2013) 1257–1261.
[16] J. Jung, et al., Electronic structures of CO adsorbed Pt-skin surface on Pt–Co and Pt–Ni alloys, Curr. Appl. Phys. 35 (2022) 1–6.
[17] W.J. Kim, et al., Electronic structure of heavy halogen atoms adsorbed on the Cu (111) surface: a combined ARPES and first principles calculations study, J. Phys. Chem. C 123 (2019) 26309–26314.
[18] S.D. Kevan, Observation of a new surface state on Cu(001), Phys. Rev. B 28 (1983) 2268–2270.
[19] K.K. Gomes, W. Mar, W. Ko, F. Guinea, H.C. Manoharan, Designer dirac fermions and topological phases in molecular graphene, Nature 483 (2012) 306–310.
[20] A. Kar, A. Das, S.R. Mohanty, S. Narasimhan, K.S.R. Menon, Evolution of geometric and electronic structures of oxygen-induced superstructures on Mo (110) surface: a LEED, ARPES, and DFT study, Phys. Rev. B 106 (2022) 045128.
[21] K. Kim, et al., Large anomalous Hall current induced by topological nodal lines in a ferromagnetic van der Waals semimetal, Nat. Mater. 17 (2018) 794–799.
[22] S. Sakong, A. Groß, The electric double layer at metal-water interfaces revisited based on a charge polarization scheme, J. Chem. Phys. 149 (2018) 084705.
[23] C. Zhang, T. Sayer, J. Hutter, M. Sprik, Modelling electrochemical systems with finite field molecular dynamics, J. Phys. Energy 2 (2020) 032005.
[24] A. Groß, S. Sakong, Modelling the electric double layer at electrode/electrolyte interfaces, Current Opin. Electrochem. 14 (2019) 1–6.
[25] W. Schmickler, Double layer theory, J. Solid State Electrochem. 24 (2020) 2175–2176.
[26] W. Schmickler, The electronic response of the metal in simulations of the electric double layer, J. Electroanal. Chem. 856 (2020) 113664.
[27] A. Ignaczak, et al., Oxygen reduction in alkaline Media - a discussion, Electrocatalysis 8 (2017) 554–564.
[28] E. Santos, W. Schmickler, Fundamental aspects of electrocatalysis, Chem. Phys. 332 (2007) 39–47.
[29] D.E. Starr, Z. Liu, M. Hävecker, A. Knop-Gericke, H. Bluhm, Investigation of solid/vapor interfaces using ambient pressure X-ray photoelectron spectroscopy, Chem. Soc. Rev. 42 (2013) 5833–5857.
[30] V.N. Strocov, C. Cancellieri, A.S. Mishchenko, Electrons and polarons at oxide interfaces explored by soft-X-ray ARPES, in: C. Cancellieri, V.N. Strocov (Eds.), Spectroscopy of Complex Oxide Interfaces: Photoemission and Related Spectroscopies, Springer International Publishing, Cham, 2018, pp. 107–151, https://doi.org/10.1007/978-3-319-74989-1_6.
[31] P.D.C. King, et al., Quasiparticle dynamics and spin–orbital texture of the SrTiO3 two-dimensional electron gas, Nat. Commun. 5 (2014) 3414.
[32] Z. Wang, et al., Anisotropic two-dimensional electron gas at SrTiO3(110), Proc. Natl. Acad. Sci. 111 (2014) 3933–3937.
[33] C. Chen, J. Avila, E. Frantzeskakis, A. Levy, M.C. Asensio, Observation of a two-dimensional liquid of Fröhlich polarons at the bare SrTiO3 surface, Nat. Commun. 6 (2015) 8585.
[34] B. Sohn, et al., Sign-tunable anomalous Hall effect induced by two-dimensional symmetry-protected nodal structures in ferromagnetic perovskite thin films, Nat. Mater. 20 (2021) 1643–1649.
[35] P.D.C. King, et al., Atomic-scale control of competing electronic phases in ultrathin LaNiO3, Nat. Nanotechnol. 9 (2014) 443–447.
[36] A.R. Akbashev, et al., Probing the stability of SrIrO3 during active water electrolysis via Operando Atomic Force microscopy, Energy Environ. Sci. 16 (2023) 513–522.
[37] J. Bosse, et al., Molecular O2 dimers and lattice instability in a perovskite electrocatalyst, J. Am. Chem. Soc. 146 (2024) 23989–23997.
[38] K.J. May, et al., Influence of oxygen evolution during water oxidation on the surface of perovskite oxide catalysts, J. Phys. Chem. Lett. 3 (2012) 3264–3270.
[39] F. Calle-Vallejo, J.I. Martínez, J.M. García-Lastra, M. Mogensen, J. Rossmeisl, Trends in stability of perovskite oxides, Angewandte Chemie Int. Ed. 49 (2010) 7699–7701.
[40] C. Baeumer, et al., Tuning electrochemically driven surface transformation in atomically flat $LaNiO_3$ thin films for enhanced water electrolysis, Nat. Mater. (2021), https://doi.org/10.1038/s41563-020-00877-1.
[41] A. Varykhalov, 1^2-ARPES: the ultra high resolution photoemission station at the U112-PGM-2a-1^2 beamline at BESSY II, J. Large-Scale Research Facil. JLSRF 4 (2018). A128–A128.
[42] H.K. Yoo, et al., Latent instabilities in metallic LaNiO3 films by strain control of fermi-surface topology, Sci. Rep. 5 (2015) 8746.
[43] A. Grimaud, et al., Activation of surface oxygen sites on an iridium-based model catalyst for the oxygen evolution reaction, Nature Energy 2 (2016) 16189.
[44] L. Yang, et al., Efficient oxygen evolution electrocatalysis in acid by a perovskite with face-sharing IrO_6 octahedral dimers, Nat. Commun. 9 (2018) 5236.
[45] J.T. Mefford, et al., Correlative operando microscopy of oxygen evolution electrocatalysts, Nature 593 (2021) 67–73.
[46] K. Schweinar, B. Gault, I. Mouton, O. Kasian, Lattice oxygen exchange in rutile IrO_2 during the oxygen evolution reaction, J. Phys. Chem. Lett. 11 (2020) 5008–5014.
[47] A. Grimaud, et al., Activating lattice oxygen redox reactions in metal oxides to catalyse oxygen evolution, Nat. Chem. 9 (2017) 457–465.
[48] J.S. Yoo, Y. Liu, X. Rong, A.M. Kolpak, Electronic origin and kinetic feasibility of the lattice oxygen participation during the oxygen evolution reaction on perovskites, J. Phys. Chem. Lett. 9 (2018) 1473–1479.
[49] C. Spöri, J.T.H. Kwan, A. Bonakdarpour, D.P. Wilkinson, P. Strasser, The stability challenges of oxygen evolving catalysts: towards a common fundamental understanding and mitigation of catalyst degradation, Angewandte Chemie Int. Ed. 56 (2017) 5994–6021.
[50] E. Fabbri, et al., Dynamic surface self-reconstruction is the key of highly active perovskite nano-electrocatalysts for water splitting, Nat Mater 16 (2017) 925.
[51] S.H. Chang, et al., Functional links between stability and reactivity of strontium ruthenate single crystals during oxygen evolution, Nat. Commun. 5 (2014) 4191.
[52] L. Trotochaud, S.L. Young, J.K. Ranney, S.W. Boettcher, Nickel–Iron oxyhydroxide oxygen-evolution electrocatalysts: the role of intentional and incidental iron incorporation, J. Am. Chem. Soc. 136 (2014) 6744–6753.
[53] P.P. Lopes, et al., Dynamically stable active sites from surface evolution of perovskite materials during the oxygen evolution reaction, J. Am. Chem. Soc. 143 (2021) 2741–2750.
[54] C. Baeumer, et al., Carbonate formation lowers the electrocatalytic activity of perovskite oxides for water electrolysis, J. Mater. Chem. A 9 (2021), 19940–19948.
[55] I. Källquist, et al., Advances in studying interfacial reactions in rechargeable batteries by photoelectron spectroscopy, J. Mater. Chem. A 10 (2022) 19466–19505.
[56] S. Patil, et al., ARPES view on surface and bulk hybridization phenomena in the antiferromagnetic Kondo lattice $CeRh_2Si_2$, Nat. Commun. 7 (2016) 11029.
[57] G. Berner, et al., Direct k-space mapping of the electronic structure in an oxide-oxide interface, Phys. Rev. Lett. 110 (2013) 247601.
[58] Q.Y. Chen, et al., Direct observation of how the heavy-fermion state develops in $CeCoIn_5$, Phys. Rev. B 96 (2017) 045107.
[59] S. Nemšák, et al., Observation by resonant angle-resolved photoemission of a critical thickness for 2-dimensional electron gas formation in $SrTiO_3$ embedded in $GdTiO_3$, Appl. Phys. Lett. 107 (2015) 231602.
[60] M. Kobayashi, et al., Unveiling the impurity band induced ferromagnetism in the magnetic semiconductor (Ga,Mn)As, Phys. Rev. B 89 (2014) 205204.
[61] V.N. Strocov, et al., k-resolved electronic structure of buried heterostructure and impurity systems by soft-X-ray ARPES, J. Electron. Spectros Relat Phenomena 236 (2019) 1–8.
[62] A. Chikina, et al., Orbital ordering of the mobile and localized electrons at oxygen-deficient LaAlO3/SrTiO3 interfaces, ACS Nano 12 (2018) 7927–7935.
[63] D. Takegami, et al., Valence band hard x-ray photoelectron spectroscopy on $3d$ transition-metal oxides containing rare-earth elements, Phys. Rev. B 99 (2019) 165101.
[64] C. Kalha, et al., Hard x-ray photoelectron spectroscopy: a snapshot of the state-of-the-art in 2020, J. Phys. Condensed Matter 33 (2021) 233001.
[65] M. Zapf, et al., Hard x-ray angle-resolved photoemission from a buried high-mobility electron system, Phys. Rev. B 106 (2022) 125137.
[66] A.X. Gray, et al., Probing bulk electronic structure with hard X-ray angle-resolved photoemission, Nat Mater 10 (2011) 759–764.
[67] J. Falke, et al., Electronic structure of the metallic oxide ${\mathrm{ReO}}_{3}$, Phys. Rev. B 103 (2021) 115125.
[68] P. Narang, C.A.C. Garcia, C. Felser, The topology of electronic band structures, Nat. Mater. 20 (2021) 293–300.
[69] J.S. Kang, S.-D. Sohn, H.-J. Shin, Dissociative adsorption of H_2O_2 on the TiO_2(110) surface for advanced oxidation process, J. Phys. Chem. C 124 (2020) 11930–11934.
[70] C.M. Lousada, A.J. Johansson, T. Brinck, M. Jonsson, Mechanism of H_2O_2 decomposition on transition metal oxide surfaces, J. Phys. Chem. C 116 (2012) 9533–9543.
[71] V. Jovic, et al., How indium nitride senses water, Nano Lett. 17 (2017) 7339–7344.
[72] M. Caputo, et al., Manipulating the topological interface by molecular adsorbates: adsorption of Co-phthalocyanine on Bi_2Se_3, Nano Lett. 16 (2016) 3409–3414.
[73] G. Wan, et al., Amorphization mechanism of $SrIrO_3$ electrocatalyst: how oxygen redox initiates ionic diffusion and structural reorganization, Sci. Adv. 7 (2021) eabc7323.
[74] P. Corbae, et al., Observation of spin-momentum locked surface states in amorphous Bi2Se3, Nat. Mater. 22 (2023) 200–206.
[75] A.-T. Tran, F. Huet, K. Ngo, P. Rousseau, Artefacts in electrochemical impedance measurement in electrolytic solutions due to the reference electrode, Electrochim. Acta 56 (2011) 8034–8039.
[76] M. Muntwiler, et al., Surface science at the PEARL beamline of the Swiss Light Source, J. Synchrotron. Radiat. 24 (2017) 354–366.
[77] W. Sugimoto, H. Iwata, K. Yokoshima, Y. Murakami, Y. Takasu, Proton and electron conductivity in hydrous ruthenium oxides evaluated by electrochemical impedance spectroscopy: the origin of large capacitance, J. Phys. Chem. B 109 (2005) 7330–7338.
[78] J. Huang, Diffusion impedance of electroactive materials, electrolytic solutions and porous electrodes: warburg impedance and beyond, Electrochim. Acta 281 (2018) 170–188.

[79] D.Y. Chung, et al., Dynamic stability of active sites in hydr(oxy)oxides for the oxygen evolution reaction, Nature Energy 5 (2020) 222–230.
[80] E. Lundgren, et al., Novel *in situ*situ techniques for studies of model catalysts, Acc. Chem. Res 50 (2017) 2326–2333.
[81] Y. Liu, T. Kawaguchi, M.S. Pierce, V. Komanicky, H. You, Layering and ordering in electrochemical double layers, J. Phys. Chem. Lett. 9 (2018) 1265–1271.
[82] G.S. Harlow, et al., Adsorption, surface relaxation and electrolyte structure at Pt (111) electrodes in non-aqueous and aqueous acetonitrile electrolytes, Phys. Chem. Chem. Phys. 21 (2019) 8654–8662.
[83] T. Fuchs, et al., Structure dependency of the atomic-scale mechanisms of platinum electro-oxidation and dissolution, Nature Catal. 3 (2020) 754–761.
[84] T. Kawaguchi, et al., Stern layers on RuO_2 (100) and (110) in electrolyte: surface X-ray scattering studies, J. Electroanal. Chem. 875 (2020) 114228.
[85] M.V. Kuznetsov, et al., Photoelectron diffraction and holography studies of 2D materials and interfaces, J. Phys. Soc. Jpn. 87 (2018) 061005.
[86] K.A. Bokai, et al., Hybrid h-BN–Graphene monolayer with B–C boundaries on a lattice-matched surface, Chem. Mater. 32 (2020) 1172–1181.
[87] F. Grillo, R. Megginson, D. Batchelor, M. Muntwiler, C.J. Baddeley, Structural and electronic characterization of Cu/Au(111) near-surface alloys, Jpn. J. Appl. Phys. 58 (SIIB09) (2019).
[88] P. Krüger, F. Da Pieve, J. Osterwalder, Real-space multiple scattering method for angle-resolved photoemission and valence-band photoelectron diffraction and its application to Cu(111), Phys. Rev. B 83 (2011) 115437.
[89] A.S. Kilian, et al., Atomic structure of Cr_2O_3/Ag(111) and Pd/Cr_2O_3/Ag(111) surfaces: a photoelectron diffraction investigation, J. Phys. Chem. C 118 (2014) 20452–20460.
[90] T. Jaouen, et al., Induced work function changes at Mg-doped MgO/Ag(001) interfaces: combined auger electron diffraction and density functional study, Phys. Rev. B 90 (2014) 125433.
[91] A. Chassé, T. Chassé, Theory and application of photoelectron diffraction for complex oxide systems, J. Phys. Soc. Jpn. 87 (2018) 061006.
[92] A. Pancotti, N. Barrett, L.F. Zagonel, G.M. Vanacore, Multiple scattering x-ray photoelectron diffraction study of the $SrTiO_3$(100) surface, J. Appl. Phys. 106 (2009) 034104.
[93] A. Berlich, H. Strauss, C. Langheinrich, A. Chassé, H. Morgner, Surface termination of $BaTiO_3$ (001) single crystals: a combined electron spectroscopic and theoretical study, Surf Sci. 605 (2011) 158–165.
[94] J.T. Diulus, et al., h-BN/metal-oxide interface grown by intercalation: a model system for nano-confined catalysis, J. Phys. Chem. C 128 (2024) 5156–5167.
[95] T. Matsushita, et al., Reconstruction algorithm for atomic-resolution holography using translational symmetry, Phys. Rev. B 78 (2008) 144111.
[96] T. Matsushita, Atomic image reconstruction from Atomic resolution holography using L1-regularized linear regression, e-J. Surface Sci. Nanotechnol. 14 (2016) 158–160.
[97] T. Matsushita, et al., Principle and reconstruction algorithm for atomic-resolution holography, J. Phys. Soc. Jpn. 87 (2018) 061002.
[98] R.H. Temperton, et al., Dip-and-pull ambient pressure photoelectron spectroscopy as a spectroelectrochemistry tool for probing molecular redox processes, J. Chem. Phys. 157 (2022) 244701.
[99] D. Teschner, et al., Understanding anomalous gas-phase peak shifts in dip-and-pull ambient pressure XPS experiments, J. Phys. Chem. C 128 (2024) 7096–7105.
[100] C. Lawley, et al., Protagonists and spectators during photocatalytic solar water splitting with SrTaOxNy oxynitride, J. Mater. Chem. A 10 (2022) 2374–2387.
[101] T. Yajima, et al., Controlling band alignments by artificial interface dipoles at perovskite heterointerfaces, Nat. Commun. 6 (2015) 6759.